

1 Evolution of irreversible somatic differentiation

2 Yuanxiao Gao¹, Hye Jin Park^{1, 2, 3}, Arne Traulsen¹, and Yuriy Pichugin¹

3 ¹Max Planck Institute for Evolutionary Biology, August-Thienemann-Str. 2,
4 24306 Plön, Germany

5 ²Asia Pacific Center for Theoretical Physics, Pohang, 37673, Korea

6 ³Department of Physics, POSTECH, Pohang, 37673, Korea

7 January 19, 2021

8 **Abstract**

9 A key innovation emerging in complex animals is irreversible somatic differentiation:
10 daughters of a vegetative cell perform a vegetative function as well, thus, forming a so-
11 matic lineage that can no longer be directly involved in reproduction. Primitive species
12 use a different strategy: vegetative and reproductive tasks are separated in time rather
13 than in space. Starting from such a strategy, how is it possible to evolve life forms which
14 use some of their cells exclusively for vegetative functions? Here, we developed an evo-
15 lutionary model of development of a simple multicellular organism and found that three
16 components are necessary for the evolution of irreversible somatic differentiation: (i)
17 costly cell differentiation, (ii) vegetative cells that significantly improve the organism's
18 performance even if present in small numbers, and (iii) large enough organism size. Our
19 findings demonstrate how an egalitarian development typical for loose cell colonies can
20 evolve into germ-soma differentiation dominating metazoans.

21 **1 Introduction**

22 In complex multicellular organisms, different cells specialise to execute different functions.
23 These functions can be generally classified into two kinds: reproductive and vegetative. Cells

24 performing reproductive functions contribute to the next generation of organisms, while cells
25 performing vegetative function contribute to sustaining the organism itself. In unicellular
26 species and simple multicellular colonies, these two kinds of functions are performed at dif-
27 ferent times by the same cells – specialization is temporal. In more complex multicellular
28 organisms, specialization transforms from temporal to spatial Mikhailov et al. [2009], where
29 groups of cells focused on different tasks emerge in the course of organism development.

30 Typically, cell functions are changed via differentiation, such that a daughter cell per-
31 forms a different function than the maternal cell. The vast majority of metazoans feature a
32 very specific and extreme pattern of cell differentiation: any cell performing vegetative func-
33 tions forms a somatic lineage, i.e. producing cells performing the same vegetative function –
34 somatic differentiation is irreversible. Since such somatic cells cannot give rise to reproduc-
35 tive cells, somatic cells do not have a chance to pass their offspring to the next generation of
36 organisms. Such a mode of organism development opened a way for deeper specialization of
37 somatic cells and consequently to the astonishing complexity of multicellular metazoans. In
38 *Volvocales* – a group of green algae serving as a model species for evolution of multicellu-
39 larity – the emergence of irreversibly differentiated somatic cells is the hallmark innovation
40 marking the transition from colonial life forms to multicellular species Kirk [2005].

41 While the production of individual cells specialized in vegetative functions comes with a
42 number of benefits Grosberg and Strathmann [2007], the development of a dedicated vegeta-
43 tive cell lineage that is lost for organism reproduction is not obviously a beneficial adaptation.
44 From the perspective of a cell in an organism, the guaranteed termination of its lineage seems
45 the worst possible evolutionary outcome for itself. From the perspective of entire organ-
46 ism, the death of somatic cell at the end of the life cycle is a waste of resources, as these cells
47 could in principle become parts of the next generation of organisms. For example, exceptions
48 from irreversible somatic differentiation are widespread in plants Lanfear [2018] and are even
49 known in simpler metazoans among cnidarians DuBuc et al. [2020] for which differentiation
50 from vegetative to reproductive functions has been reported. Therefore, the irreversibility of
51 somatic differentiation cannot be taken for granted in the course of the evolution of complex

52 multicellularity.

53 The majority of the theoretical models addressing the evolution of somatic cells focuses
54 on the evolution of cell specialization, abstracting from the developmental process how germ
55 (reproductive specialists) and soma are produced in the course of the organism growth. For
56 example, a large amount of work focuses on the optimal distribution of reproductive and
57 vegetative functions in the adult organism Michod [2007], Willensdorfer [2009], Rossetti
58 et al. [2010], Rueffler et al. [2012], Ispolatov et al. [2012], Goldsby et al. [2012], Solari
59 et al. [2013], Goldsby et al. [2014], Amado et al. [2018], Tverskoi et al. [2018]. However,
60 these models do not consider the process of organism development. Other work takes the
61 development of an organism into account to some extent: In Gavrilets [2010], the organism
62 development is considered, but the fraction of cells capable to become somatic is fixed and
63 does not evolve. In Erten and Kokko [2020], the strategy of germ-to-soma differentiation is
64 an evolvable trait, but the irreversibility of somatic differentiation is taken for granted. In
65 Rodrigues et al. [2012], irreversible differentiation was found, but both considered cell types
66 pass to the next generation of organisms, such that the irreversible specialists are not truly
67 somatic cells in the sense of evolutionary dead ends. Finally, in Cooper and West [2018]
68 all model ingredients are present: the strategy of cell differentiation is explicitly considered
69 and it is an evolvable trait, also soma and germ cells are considered. However, irreversible
70 somatic differentiation was not observed in that study. Hence, the theoretical understanding
71 of the evolution of irreversibly differentiated somatic cell lines is limited so far.

72 We developed a theoretical model to investigate conditions for the evolution of the irre-
73 versible somatic differentiation, in which vegetative soma-role cells are, in principle, capable
74 to re-differentiate and produce reproductive germ-role cells. In our model, we incorporate
75 factors including (i) costs of cell differentiation, (ii) benefits provided by presence of soma-
76 role cells, (iii) maturity size of the organism. We ask under which circumstances irreversible
77 somatic differentiation is a strategy that can maximize the population growth rate compared
78 to strategies in which differentiation does not occur or somatic differentiation is reversible.

79 2 Model

80 We consider a large population of clonally developing organisms composed of two types of
81 cells: germ-role and soma-role. Each organism is initiated as a single germ-role cell. In
82 the course of the organism growth, germ-role cells may differentiate to give rise to soma-
83 role cells and vice versa, see Fig. 1A,B. We assume that somatic cells accelerate growth: an
84 organism containing more somatic cells grows faster. After n rounds of synchronous cell
85 divisions, the organism reaches its maturity size of 2^n cells. Immediately upon reaching
86 maturity, the organism reproduces: germ-role cells disperse and each becomes a newborn
87 organism, while all soma-role cells die and are thus lost, see Fig. 1A.

88 To investigate the evolution of irreversible somatic differentiation, we consider organisms
89 in which the functional role of the cell (germ-role or soma-role) is not necessarily inherited.
90 When a cell divides, the two daughter cells can change their role, leading to three possi-
91 ble combinations: two germ-role cells, one germ-role cell plus one soma-role cell, or two
92 soma-role cells. We allow all these outcomes to occur with different probabilities, which also
93 depend on the parental type, see Fig 1B. If the parental cell had the germ-role, the probabil-
94 ities of each outcome are denoted by g_{gg} , g_{gs} , and g_{ss} respectively. If the parental cell had
95 the soma-role, these probabilities are s_{gg} , s_{gs} , and s_{ss} . Altogether, six probabilities define
96 a stochastic developmental strategy $D = (g_{gg}, g_{gs}, g_{ss}; s_{gg}, s_{gs}, s_{ss})$. In our model, it is the
97 stochastic developmental strategy that is inherited by offspring cells rather than the functional
98 role of the parental cell.

99 To feature irreversible somatic differentiation (ISD in the following), the developmental
100 strategy must allow germ-role cells to give rise to soma-role cells ($g_{gg} < 1$) and must forbid
101 soma-role cells to give rise to germ-role cells ($s_{ss} = 1$). All other developmental strategies
102 can be broadly classified into two classes. Reversible somatic differentiation (RSD) describes
103 strategies where cells of both roles can give rise to each other: $g_{gg} < 1$ and $s_{ss} < 1$. In the
104 strategy with no somatic differentiation (NSD), soma-role cells are not produced in the first
105 place: $g_{gg} = 1$, see Table 1.

106 In our model, evolution is driven by the growth competition between populations ex-

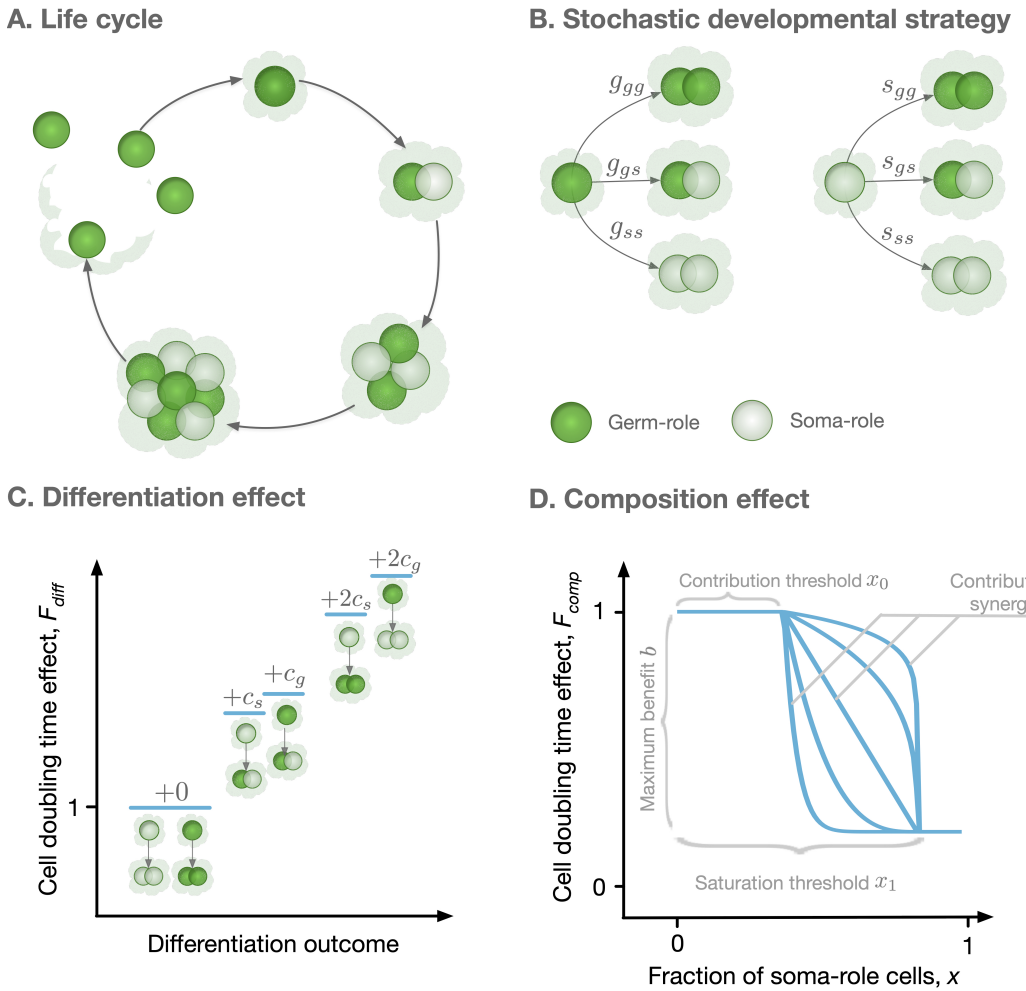


Figure 1: Model overview. **A.** The life cycle of an organism starts with a single germ-role cell. In each round, all cells divide and daughter cells can differentiate into a role different from the maternal cell's role. When the organism reaches maturity, it reproduces: each germ-role cell becomes a newborn organism and each soma-role cell dies. **B.** Change of cell roles is controlled by a stochastic developmental strategy defined by probabilities of each possible outcomes of a cell division. **C.** Differentiation of cells requires an investment of resources and, thus, slows down the organism growth. Each cell differentiation event incurs a cost (c_s or c_g). The average cost of differentiation contributes increases the cell doubling time in a multiplicative way. **D.** The growth contribution of somatic cells is controlled by a function that decreases the doubling time with the fraction of somatic cells. The form of this function is controlled by four parameters, x_0 , x_1 , α , and b .

Table 1: Classification of developmental strategies

Class	Label	g_{gg}	s_{ss}
Irreversible somatic differentiation	ISD	< 1	$= 1$
Reversible somatic differentiation	RSD	< 1	< 1
No somatic differentiation	NSD	$= 1$	irrelevant

107 executing different developmental strategies. Growth competition will favour developmental
 108 strategies that lead to faster growth Pichugin et al. [2017], Gao et al. [2019]. The rate of pop-
 109 ulation growth is determined by the number of offspring produced by an organism (equal to
 110 the number of germ-role cells at the end of life cycle) and the time needed for an organism to
 111 develop from a single cell to maturity (improved with the number of soma-role cells during
 112 the life cycle). The development consists of n rounds of simultaneous cell divisions. Conse-
 113 quently, the total development time is a sum of n time intervals between cell doubling events.
 114 Each cell doubling time t is determined by two independent effects: the differentiation effect
 115 F_{diff} representing costs of changing cell roles Gallon [1992] and the organism composition ef-
 116 fect F_{comp} representing benefits from having soma-role cells Grosberg and Strathmann [1998,
 117 2007], Shelton et al. [2012], Matt and Umen [2016],

$$t = F_{\text{diff}} \times F_{\text{comp}}. \quad (1)$$

118 The cell differentiation effect F_{diff} represents the costs of cell differentiation. The differ-
 119 entiation of a cell requires efforts to modify epigenetic marks in the genome, recalibration
 120 of regulatory networks, synthesis of additional and utilization of no longer necessary pro-
 121 teins. This requires an investment of resources and therefore an additional time to perform
 122 cell division. Hence, any cell, which is about to give rise to a cell of a different role, incurs
 123 a differentiation costs c_g for germ-to-soma and c_s for soma-to-germ transitions, see Fig. 1C.
 124 The resulting effect of differentiation costs is determined as $F_{\text{diff}} = 1 + \langle c \rangle$, where $\langle c \rangle$ is the
 125 average differentiation cost among all cells in an organism.

126 The composition effect profile $F_{\text{comp}}(x)$ captures how the cell division time depends on
 127 the proportion of soma-role cells x present in an organism. In this study, we use a functional

¹²⁸ form illustrated in Fig. 1D and given by

$$F_{\text{comp}}(x) = \begin{cases} 1 & \text{for } 0 \leq x \leq x_0 \\ 1 - b + b \left(\frac{x_1 - x}{x_1 - x_0} \right)^\alpha & \text{for } x_0 < x < x_1 \\ 1 - b & \text{for } x_1 \leq x \leq 1 \end{cases} \quad (2)$$

¹²⁹ With the functional form (2), soma-role cells can benefit to the organism growth, only if their
¹³⁰ proportion in the organism exceeds the contribution threshold x_0 . Interactions between soma-
¹³¹ role cells may lead to the synergistic (soma-role cells work better together than alone), or
¹³² discounting benefits (soma-role cells work better alone than together) to the organism growth,
¹³³ controlled by the contribution synergy parameter α . The maximal achievable reduction in the
¹³⁴ cell division time is given by the maximal benefit b , realized beyond the saturation threshold
¹³⁵ x_1 of the soma-role cell proportion. A further increase in the proportion of soma-role cells
¹³⁶ does not provide any additional benefits. With the right combination of parameters, (2) is able
¹³⁷ to recover various characters of soma-role cells contribution to the organism growth: linear
¹³⁸ ($x_0 = 0, x_1 = 1, \alpha = 1$), power-law ($x_0 = 0, x_1 = 1, \alpha \neq 1$), step-functions ($x_0 = x_1$), and a
¹³⁹ huge range of other scenarios.

¹⁴⁰ For a given combination of differentiation costs (c_g, c_s) and a composition effect profile
¹⁴¹ (determined by four parameters: x_0, x_1, b , and α), we screen through a number of stochastic
¹⁴² developmental strategies D and identify the one providing the largest growth rate to the pop-
¹⁴³ ulation. In this study, we searched for those parameters under which ISD strategies lead to
¹⁴⁴ the fastest growth and are thus evolutionary optimal, see model details in Appendix A.1.

¹⁴⁵ 3 Results

¹⁴⁶ 3.1 For irreversible somatic differentiation to evolve, cell differentiation ¹⁴⁷ must be costly.

¹⁴⁸ We found that irreversible somatic differentiation (ISD) does not evolve when cell differenti-
¹⁴⁹ ation is not associated with any costs ($c_s = c_g = 0$), see Fig 2A. This finding comes from the

150 fact that when somatic differentiation is irreversible, the fraction of germ-role cells can only
151 decrease in the course of life cycle. As a result, ISD strategies deal with the tradeoff between
152 producing more soma-role cells at the beginning of the life cycle, and having more germ-role
153 cells by the end of it. On the one hand, ISD strategies which produce a lot of soma-role cells
154 early on, complete the life cycle quickly but preserve only a few germ-role cells by the time
155 of reproduction. On the other hand, ISD strategies which generate a lot of offspring, can
156 deploy only a few soma-role cells at the beginning of it and thus their developmental time
157 is inevitably longer. By contrast, reversible somatic differentiation strategies (RSD) do not
158 experience a similar tradeoff, as germ-role cells can be generated from soma-role cells. As a
159 result, RSD allows higher differentiation rates and can develop a high soma-role cell fraction
160 in the course of the organism growth and at the same time have a large number of germ-role
161 cells by the moment of reproduction. Under costless cell differentiation, for any ISD strat-
162 egy, we can find an RSD counterpart, which leads to faster growth: the development proceeds
163 faster, while the expected number of produced offspring is the same, see Appendix A.2for
164 details. As a result, costless cell differentiation cannot lead to irreversible somatic differenti-
165 ation.

166 To confirm the reasoning that RSD strategies gain an edge over ISD by having larger
167 differentiation rates, we asked which ISD and RSD strategies become optimal at various cell
168 differentiation costs ($c_s = c_g$). At each value of costs, we found evolutionarily optimal devel-
169 opmental strategy for 3000 different randomly sampled composition effect profiles $F_{\text{comp}}(x)$.
170 We found that evolutionarily optimal RSD strategies feature much larger rates of cell differ-
171 entiation than evolutionarily optimal ISD strategies, see Fig. 2B. Even at large costs, where
172 frequent differentiation is heavily penalized, the distinction between differentiation rates of
173 ISD and RSD strategies remains apparent.

174 We screened through a spectrum of germ-to-soma (c_g) and soma-to-germ (c_s) differen-
175 tiation costs, see Fig 2A. Both differentiation costs punish RSD strategies severely due to
176 their high differentiation rates. By contrast, strategies with irreversible somatic differentia-
177 tion are insensitive to changes in soma-to-germ differentiation costs c_s , because soma-role

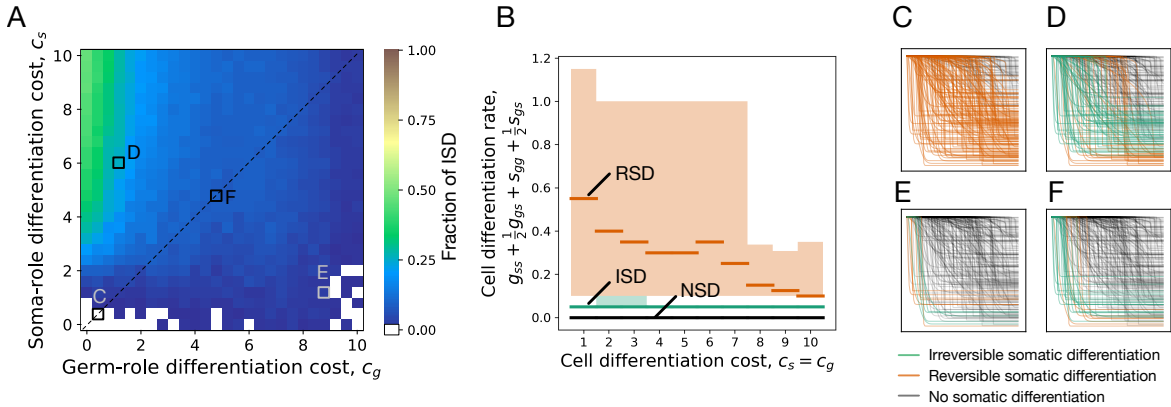


Figure 2: Irreversible soma evolves when cell differentiation is costly. **A.** The fraction of composition effect profiles, (2), promoting ISD as a function of the differentiation costs c_g and c_s . We randomly draw the parameters in (2) to construct 200 random profiles (see Appendix for details). The absence of costs ($c_g = c_s = 0$) as well as large costs of germ differentiation (large c_g) suppresses the evolution of ISD. Irreversible somatic differentiation is promoted most when the cell differentiation cost is large for soma-role cells (c_s) and small for germ-role cells (c_g). The maturity size used in the calculation is 2^{10} cells. Black dashed lines at panel B indicates the line of equal costs $c_s = c_g$ and squares indicate the costs shown in panels C-F. **B.** Cumulative cell differentiation rate ($g_{ss} + \frac{1}{2}g_{gs} + s_{ss} + \frac{1}{2}s_{gs}$) in developmental strategies evolutionarily optimal at various differentiation costs ($c_s = c_g$), separated by class (ISD, RSD, or NSD). Thick lines represent median values within each class, shaded areas show 90% confidence intervals. For each cost value, 3000 random profiles are used. Evolutionary optimal RSD strategies (orange) have much higher rates of cell differentiation than ISD (green). Consequently, RSD is penalized more under costly differentiation. **C - F.** Shapes of composition effect profiles (compare Fig. 1D) promoting ISD (green lines), RSD (orange lines), and NSD (black lines) developmental strategies at four parameter sets indicated in panel A.

178 cells never give rise to germ-role cells in ISD. Consequently, we observed that ISD is most
179 likely to evolve, when the transition from germ-role to soma-role is cheap (c_g is small) and
180 the reverse transition is expensive (c_s is large), see Fig 2A. In a similar manner, an increase
181 in germ-to-soma differentiation costs (c_g) punishes both RSD and ISD strategies. However,
182 RSD strategies tend to have larger rates of germ-to-soma transitions. Thus, they are punished
183 more than ISD, which leads to the evolution of ISD at small c_s and large c_g . Finally, the NSD
184 strategy does not pay any costs at all, as no cell differentiation occurs. Hence, at very large
185 germ-to-soma differentiation costs ($c_g \approx 10$ at Fig. 2A), the NSD strategy outcompetes both
186 reversible and irreversible somatic differentiation, see Appendix A.3 for details. For simplic-
187 ity, hereafter we focus on the case of the equal differentiation costs $c_s = c_g = c$ (a black
188 dashed line on Fig 2A).

189 **3.2 Evolution of irreversible somatic differentiation is promoted when
190 even a small number of somatic cells provides benefits to the organ-
191 ism.**

192 The composition effect profiles $F_{\text{comp}}(x)$ that promote the evolution of irreversible somatic
193 differentiation have certain characteristic shapes, see 2C-F. We investigated what kind of
194 composition effect profiles can make irreversible somatic differentiation become an evolu-
195 tionary optimum. We sampled a number of random composition effect profiles with indepen-
196 dently drawn parameter values and found optimal developmental strategies for each profile
197 for a number of differentiation costs (c) and maturity size (2^n) values. We took a closer
198 look at the instances of $F_{\text{comp}}(x)$ which resulted in irreversible somatic differentiation being
199 evolutionarily optimal.

200 We found that ISD is only able to evolve when the soma-role cells contribute to the
201 organism cell doubling time even if present in small proportions, see Fig. 3A,B. Analysing
202 parameters of the composition factors promoting ISD, we found that this effect manifests in
203 two patterns. First, the contribution threshold value (x_0) has to be small, see Fig 3D – ISD

204 is promoted when soma-role cells begin to contribute to the organism growth even in low
205 numbers. Second, the contribution synergy was found to be large ($\alpha > 1$) or, alternatively,
206 the saturation threshold (x_1) was small, see Fig 3C.

207 Both the contribution threshold x_0 and the contribution synergy α control the shape of
208 the composition effect profile at intermediary abundances of soma-role cells. If the con-
209 tribution synergy α exceeds 1, the profile is convex, so the contribution of soma-role cells
210 quickly becomes close to maximum benefit (b). A small saturation threshold (x_1) means that
211 the maximal benefit of soma is achieved already at low concentrations of soma-role cells
212 (and then the shape of composition effect profile between two close thresholds has no sig-
213 nificance). Together, these patterns give an evidence that the most crucial factor promoting
214 irreversible somatic differentiation is the effectiveness of soma-role cells at small numbers,
215 see Appendix A.4 for more detailed data presentation.

216 The reason behind these patterns is a slower accumulation of soma-role cells under irre-
217 versible somatic differentiation, comparing to RSD strategies, see Appendix A.2. Thus, with
218 ISD, an organism spends a significant amount of time having only a few soma role cells.
219 Hence, ISD strategy can only be evolutionarily successful, if these few soma-role cells have
220 a notable contribution to the organism growth time.

221 We also found that profiles featuring ISD do not possess neither extremely large, nor
222 extremely small maximal benefit values b , see Fig. 3D. When the maximal benefit is too
223 small, the cell differentiation just does not provide enough benefits to be selected for and
224 the evolutionarily optimal strategy is NSD. In the opposite case, when the maximal benefit
225 is very close to one, the cell doubling time approaches zero, see (2). Then, the benefits of
226 having many soma-role cells outweighs the costs of differentiation and the optimal strategy
227 is RSD, see Appendix A.4.

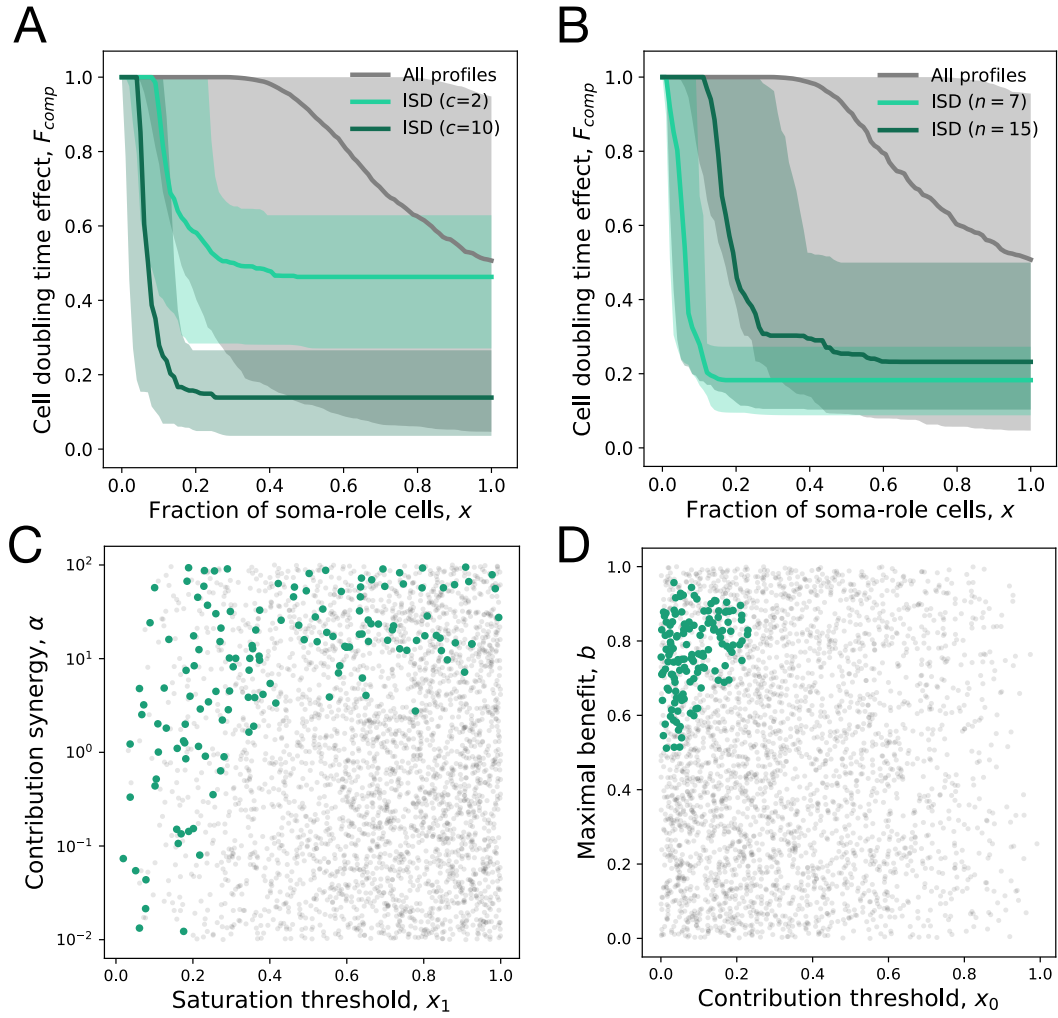


Figure 3: Irreversible soma evolves when substantial benefits arise at small concentrations of soma-role cells. In all panels, the data representing the entire set of composition effect profiles $F_{\text{comp}}(x)$ is presented in grey, while the subset promoting ISD is coloured. **A, B.** Median and 90% confidence intervals of composition effect profiles at different differentiation costs (**A**, maturity size $n = 10$) and maturity sizes (**B**, differentiation costs $c = 5$). **C, D.** The set of composition effect profiles in the parameter space. Each point represents a single profile ($c = 5$ and $n = 10$). **C.** The co-distribution of the saturation threshold (x_1) and the contribution synergy (α) reveals that either x_1 must be small or α must be large. **D.** Co-distribution of the contribution threshold (x_0) and the maximal benefit (b) shows that x_0 must be small, while b must be large to promote ISD. 3000 profiles are used for panels A, C, D and 1000 profiles for panel B.

228 **3.3 For irreversible somatic differentiation to evolve, the organism size**
229 **must be large enough.**

230 By screening through the maturity size (2^n) and differentiation costs (c), we found that the
231 evolution of irreversible somatic differentiation is heavily suppressed at small maturity sizes,
232 Fig 4A. For $c_s = c_g$, the minimal maturity size allowing irreversible somatic differentiation
233 to evolve is $2^n = 64$ cells. At the same time, organisms performing just a few more rounds
234 of cell divisions are able to evolve ISD at a wide range of cell differentiation costs, see also
235 Appendix A.5. This indicates that the evolution of irreversible somatic differentiation is
236 strongly tied to the size of the organism.

237 Evolution of ISD at sizes smaller than 64 cells is possible for $c_s > c_g$. For instance, at
238 $c_s = 2c_g$ some ISD strategies were found to be optimal at the maturity size $2^5 = 32$ cells,
239 Fig 4B. However, ISD strategies were found in a narrow range of cell differentiation costs
240 and the fraction of composition effect profiles that allow evolution of ISD there was quite
241 low – about 1%. The evolution of ISD at such small maturity sizes becomes likely only at
242 extremely unequal costs of transition between germ and some roles $c_s \gg c_g$, see Fig 4C.
243 Hence, for irreversible somatic differentiation to evolve, the organism size should exceed a
244 threshold of roughly 64 cells.

245 **4 Discussion**

246 The vast majority of cells in a body of any multicellular being contains enough genetic in-
247 formation to build an entire new organism. However, in a typical metazoan species, very few
248 cells actually participate in the organism reproduction – only a limited number of germ cells
249 are capable to do it. The other cells, called somatic cells, perform vegetative functions but do
250 not try to form an offspring organism – somatic differentiation is irreversible. We asked for
251 the reason for the success of such a specific mode of organism development. We theoretically
252 investigated the evolution of irreversible somatic differentiation with a model of clonally de-
253 veloping organisms taking into account benefits provided by soma-role cells, costs arising

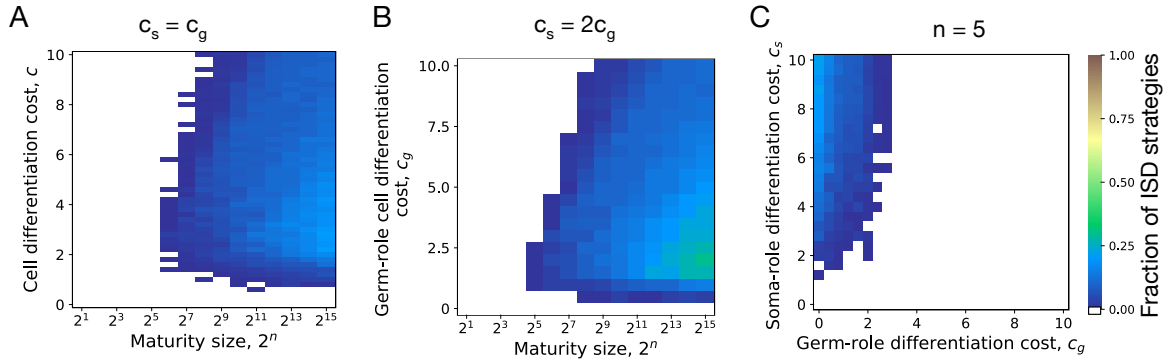


Figure 4: Irreversible soma can evolve if organism grows to a large enough size in the course of its life cycle. **A.** The fraction of composition effect profiles promoting ISD at various cell differentiation costs ($c = c_s = c_g$) and maturity sizes (2^n). ISD strategies were only found for maturity size $2^6 = 64$ cells and larger. **B.** The fraction of composition effect profiles promoting ISD at unequal differentiation costs $c_s = 2c_g$. A rare occurrences of ISD ($\sim 1\%$) was detected at the maturity size $2^5 = 32$ cells in a narrow range of cell differentiation costs but not at the smaller sizes. **C.** The range of cell differentiation costs promoting ISD at at the maturity size $2^5 = 32$ cells. For ISD strategies to evolve at such a small size, the differentiation from soma-role to germ-role must be much more costly than the opposite transition ($c_s \gg c_g$).

254 from cell differentiation, and the effect of the raw organism size.

255 While our model can capture some key features of these biological systems, it remains of
 256 course an abstraction. We assumed that populations go into an exponential growth phase –
 257 competition for space or nutrients could lead to selection of other strategies instead. Addi-
 258 tional features such as trade-offs in growth at different colony sizes lead to further complica-
 259 tions. Nevertheless, our model allows to start to look into the basic features of nascent life
 260 cycles at the edge of the division of labour in multicellular colonies.

261 Our key findings are:

262 • The evolution of irreversible somatic differentiation is inseparable from cell differenti-
 263 ation being costly.

264 ● For irreversible somatic differentiation to evolve, somatic cells should be able to con-
265 tribute to the organism performance already when their numbers are small.

266 ● Only large enough organisms tend to develop irreversible somatic differentiation.

267 According to our results, cell differentiation costs are essential for the emergence of irre-
268 versible somatic differentiation, see Fig. 2A. For cells in a multicellular organism, differen-
269 tiation costs arise from the material needs, energy, and time it takes to produce components
270 necessary for the performance of the differentiated cell, which were absent in the parent cell.
271 For instance, in filamentous cyanobacteria nitrogen-fixating heterocysts develop much thicker
272 cell wall than parent photosynthetic cells had. Also, reports indicate between 23% Ow et al.
273 [2008] and 74% Sandh et al. [2014] of the proteome changes its abundance in heterocysts
274 compared against photosynthetic cells. Similarly, the changes in the protein composition
275 in the course of cell differentiation was found during the development of stalk and fruiting
276 bodies of *Dictyostelium discoideum* Bakthavatsalam and Gomer [2010], Czarna et al. [2010]

277 Our model demonstrates that irreversible somatic differentiation is more likely to evolve
278 when a few soma-role cells are able to provide a substantial benefit to the organism, see Fig. 3.

279 Several patterns of how the benefit provided by somatic cells changes with their numbers
280 have been previously considered in the literature. However, the range of studied examples
281 was restricted to concave or convex shapes Michod [2007], Willensdorfer [2009], Rossetti
282 et al. [2010], Cooper and West [2018]. In this paper, we went beyond these shapes and
283 additionally considered lower (x_0) and upper (x_1) thresholds for the somatic cells contribution
284 (our model recovers the previous approaches for $x_0 = 0$ and $x_1 = 1$). While our findings are
285 in a qualitative agreement with these past results – the profiles promoting irreversible somatic
286 differentiation appear convex, see Fig. 3A,B – our model indicates that the crucial component
287 here is the large benefits provided by small numbers of soma-role cells, rather than overall
288 convexity of the profile. For example, with sufficiently small x_1 , the non-constant section
289 of the composition effect profile (where the fraction of soma-role cells is between x_0 and
290 x_1 , see Fig. 1D) can be concave ($\alpha < 1$, see Fig. 3C) and still promote irreversible somatic
291 differentiation. *Volvocales* algae demonstrate that a significant contribution by small numbers

292 of somatic cells might indeed be found in a natural population: In *Eudorina illinoiensis* – one
293 of the simplest species demonstrating the first signs of reproductive division of labour, only
294 four out of thirty-two cells are vegetative Sambamurti [2005] (soma-role in our terms). This
295 species has developed some reproductive division of labour and a fraction of only 1/8 of
296 vegetative cells is sufficient for colony success. Thus, it seems possible that highly-efficient
297 soma-role cells open the way to the evolution of irreversible somatic differentiation.

298 Our model shows that irreversible somatic differentiation can only emerge in relatively
299 large organisms, see Fig 4A. The maturity size plays an important role in an organism's life
300 cycle Amado et al. [2018], Erten and Kokko [2020]: Large organisms have potential advan-
301 tages to optimize themselves in multiple ways, such as to improve growth efficiency Waters
302 et al. [2010], to avoid predators Matz and Kjelleberg [2005], Fisher et al. [2016], Hiltunen
303 and Becks [2014] to increase problem-solving efficiency Morand-Ferron and Quinn [2011],
304 and to exploit the division of labour in organisms Carroll [2001], Matt and Umen [2016].
305 Moreover, the maximum size has been related to the reproduction of the organism from the
306 onset of multicellularity in Earth's history Ratcliff et al. [2012]. Our results suggest that the
307 smallest organism able to evolve irreversible somatic differentiation should typically be about
308 32 – 64 cells (unless the cost of soma-to-germ differentiation is extremely large and the cost
309 of the reverse is low). This is in line with the pattern of development observed in *Volvocales*
310 green algae. In *Volvocales*, cells are unable to move (vegetative function) and divide (re-
311 productive function) simultaneously, as a unique set of centrioles are involved in both tasks
312 Wynne and Bold [1985], Koufopanou [1994]. *Chlamydomonas reinhardtii* (unicellular) and
313 *Gonium pectorale* (small colonies up to 16 cells) perform these tasks at different times. They
314 move towards the top layers of water during the day to get more sunlight. At night, however,
315 these species perform cell division and/or colony reproduction, slowly sinking down in the
316 process. However, among larger *Volvocales*, a division of labour begins to develop. In *Eu-*
317 *dorina elegans* colonies, containing 16 - 32 cells, a few cells at the pole have their chances
318 to give rise to an offspring colony reduced Marchant [1977], Hallmann [2011]. In *Pleodo-*
319 *rina californica*, half of the 128-celled colony is formed of smaller cells, which are totally

320 dedicated to the colony movement and die at the end of colony life cycle Kikuchi [1978],
321 Hallmann [2011]. In *Volvox carteri*, most of a 10000-cell colony is formed by somatic cells,
322 which die upon the release of offspring groups Hallmann [2011].

323 Our study originated from curiosity about driving factors in the evolution of irreversible
324 somatic differentiation: Why does the green algae *Volvox* from the kingdom Plantae shed
325 most of its biomass in a single act of reproduction? And why, in another kingdom, Animalia,
326 in most of the species the majority of body cells is outright forbidden to contribute to the next
327 generation? Our results show which factors makes a difference between the evolution of an
328 irreversible somatic differentiation and other strategies of development. One of these factors,
329 the maturity size, is known in the context of the evolution of reproductive division of labour
330 Kirk [2005]. Another factor, the costs of cell differentiation, is, in general, discussed in a
331 greater biological scope but is hardly acknowledged as a factor contributing to the evolution
332 of organism development. Finally, the early contribution of soma-role cells to the organism
333 growth, even if they are small in numbers, is an unexpected outcome of our investigation,
334 overlooked so far as well. Despite the simplistic nature of our model (we did not aim to
335 model any specific organism), all our results find a confirmation among the *Volvocales* clade.
336 Hence, we expect that the findings of this study reveal general properties of the evolution of
337 irreversible somatic differentiation, independently of the clade where it evolves.

338 A Appendix

339 A.1 Search for the evolutionarily optimal developmental program

340 A.1.1 Finding the population growth rate for a given developmental program.

341 In [Gao et al., 2019], we have shown that a population of organisms, which begin their life
342 cycle from the same state but have a stochastic development, eventually grows exponentially
343 with the rate λ given by the solution of

$$\sum_i e^{-\lambda T_i} G_i P_i = 1. \quad (3)$$

344 Here, i is the developmental trajectory – in our case, the specific combination of all cell divi-
345 sion outcomes; P_i is the probability that an organism development will follow the trajectory
346 i ; T_i is the time necessary to complete the trajectory i – from a single cell to the maturity size
347 of 2^n cells; G_i is the number of offspring organisms produced at the end of developmental
348 trajectory i , equal to the number of germ-role cells at the moment of maturity.

349 In order to find the population growth rate, we need to know G_i , T_i , and P_i (how many
350 offspring are produced, how long did it take to mature, and how likely is this developmental
351 trajectory, respectively). The complete set of developmental trajectories is huge as it scales
352 exponentially with the number of divisions n .

353 In our study, for each developmental strategy, we sampled $M = 300$ developmental
354 trajectories at random. To get each trajectory, we simulated the growth of the single organism
355 according to the rules of our model. For each trajectory, the developmental time T_i was
356 computed as a sum of cell doubling times at each of the n synchronous cell divisions, the
357 number of offspring G_i was given by the count of germ-role cells at the end of development.
358 The resulting ensemble of trajectories (with $P_i = 1/M$) was plugged into (3) to compute the
359 population growth rate λ .

360 A.1.2 Finding the developmental program with the largest population growth rate

361 We assume that evolution occurs by growth competition between populations executing dif-
362 ferent developmental strategies. These strategies, which provide larger population growth
363 rate will outgrow others. To find evolutionarily optimal strategies under given conditions, we
364 screened through a large set of developmental strategies and identified the one with the max-
365 imal population growth rate λ . Since the probabilities of cell division outcomes sum into one
366 ($g_{gg} + g_{gs} + g_{ss} = 1$ and $s_{gg} + s_{gs} + s_{ss} = 1$), these probabilities can be represented as a point on
367 two simplexes, one for the division of germ-role cells, and one for the division of soma-role
368 cells. Consequently, we choose the set of developmental strategies as a Cartesian product of
369 two triangular lattices - one for division probabilities of germ-role cells (g_{gg}, g_{gs}, g_{ss}) and one
370 for soma-role cells (s_{gg}, s_{gs}, s_{ss}). The lattice space was set to 0.1, so each of two indepen-
371 dent lattices contained $11 \times 12/2 = 66$ nodes, and the whole set of developmental strategies
372 comprised $66 \times 66 = 4356$ different strategies. For each of these strategies, the population
373 growth rate λ was calculated and the strategy with the largest growth rate was identified as
374 evolutionarily optimal.

375 In our investigation, parameters such as differentiation costs (c_s, c_g) and maturity size (2^n)
376 were used as control parameters. In other words, we either fix them at the specific values,
377 or screened through a range of values to obtain a map (see Figs. 2 and 3 in the main text).
378 However, the parameters controlled the shape of composition effect profile (x_0, x_1, α , and b)
379 were treated differently. For each combination of control parameters, we randomly sampled
380 a number (between 200 and 3000) of combinations of these parameters. The thresholds
381 ($0 \leq x_0 \leq x_1 \leq 1$) were sampled as a pair of independent distributed random values from
382 the uniform distribution $U(0, 1)$. The contribution threshold x_0 was set to the minimum of
383 the pair, and the saturation threshold x_1 was set to the maximum. The contribution synergy
384 ($\alpha > 0$) corresponds to the concave shape of the profile at $\alpha < 1$ and to the convex shape
385 at $\alpha > 1$. Therefore, $\log_{10}(\alpha)$ was sampled from the uniform distribution $U(-2, +2)$, so
386 the profile has an equal probability to demonstrate concave and convex shape. Finally, the
387 maximum benefit ($0 \leq b < 1$) was sampled from a uniform distribution, $U(0, 1)$. For each

388 tested combination of control parameters, we found the optimal developmental strategy for
 389 every sampled profile. We then classified these as irreversible somatic differentiation (ISD),
 390 reversible somatic differentiation (RSD), or no somatic differentiation (NSD).

391 **A.2 Under costless cell differentiation, irreversible soma strategy can-
 392 not be evolutionarily optimal**

393 In this section, we will show that an ISD strategy can never be an evolutionary optimum with-
 394 out cell differentiation being costly. To do that, we first consider the deterministic dynamics
 395 of the expected composition of the organism. Then, for an arbitrary ISD strategy, we identify
 396 a more advantageous RSD strategy which gives the same organism composition at the end of
 397 life cycle but higher number of soma-role cells during the life cycle.

398 In our model, the composition of the organism is governed by the stochastic develop-
 399 mental strategy and differs between different organisms. Here, as a proxy for this complex
 400 stochastic dynamics, we consider the mathematical expectation of the composition. Assume
 401 that after $t \geq 0$ cell divisions the fraction of soma-role cells is $s(t)$ and the fraction of germ-
 402 role cells is $g(t) = 1 - s(t)$. Then, the expected fractions of cells of the two types after the
 403 next cell division is

$$\begin{aligned} s(t+1) &= \left(s_{ss} + \frac{s_{gs}}{2} \right) s(t) + \left(\frac{g_{gs}}{2} + g_{ss} \right) g(t) = (1 - m_s)s(t) + m_g g(t), \\ g(t+1) &= \left(g_{gg} + \frac{g_{gs}}{2} \right) g(t) + \left(\frac{s_{gs}}{2} + s_{gg} \right) s(t) = (1 - m_g)g(t) + m_s s(t), \end{aligned} \quad (4)$$

404 where we introduced $m_s = s_{gg} + \frac{s_{gs}}{2}$ and $m_g = g_{ss} + \frac{g_{gs}}{2}$ – the probabilities that the offspring
 405 of a cell will have a different role. Naturally, for irreversible somatic differentiation (ISD)
 406 $m_s = 0$ and $m_g > 0$, for NSD strategies $m_g = 0$ and m_s being irrelevant, while the reversible
 407 differentiation (RSD) class covers the rest. (4) can be written in matrix form

$$\begin{pmatrix} s(t+1) \\ g(t+1) \end{pmatrix} = \begin{pmatrix} 1 - m_s & m_g \\ m_s & 1 - m_g \end{pmatrix} \cdot \begin{pmatrix} s(t) \\ g(t) \end{pmatrix} \quad (5)$$

408 A newborn organism contains a single germ-role cell ($s(0) = 0, g(0) = 1$), therefore, the

409 expected composition of an organism after i divisions is

$$\begin{pmatrix} s(t) \\ g(t) \end{pmatrix} = \begin{pmatrix} 1 - m_s & m_g \\ m_s & 1 - m_g \end{pmatrix}^t \cdot \begin{pmatrix} 0 \\ 1 \end{pmatrix} \quad (6)$$

410 The matrix has two eigenvalues: 1 and $1 - m_g - m_s$, with associated right eigenvectors
 411 $(m_g, m_s)^T$ and $(1, -1)^T$, respectively. Hence, the expected composition after t divisions can
 412 be obtained in the explicit form

$$\begin{aligned} s(t) &= \frac{1}{m_g + m_s} [m_g - m_g(1 - m_g - m_s)^t], \\ g(t) &= \frac{1}{m_g + m_s} [m_s + m_g(1 - m_g - m_s)^t]. \end{aligned} \quad (7)$$

413 For an arbitrary irreversible somatic differentiation strategy D , $m_s = 0$, the expected
 414 number of soma-role cells changes as

$$s_D(t) = 1 - (1 - m_g)^t, \quad (8)$$

415 which is a monotonically increasing function of the number of cell divisions t , see the green
 416 line in Fig. 5. In the life cycle involving n cell divisions, the fraction of soma-role cells at the
 417 end of life cycle is $s_D(n) = 1 - (1 - m_g)^n$.

418 Now, we consider another developmental strategy D' with reversible somatic differenti-
 419 ation in which $m'_g = s_D(n)$ and $m'_s = 1 - s_D(n)$. Using $m'_g + m'_s = 1$ in (7), it can be
 420 shown that the expected fraction of soma-role cells in D' after the very first cell division is
 421 exactly $s_D(n)$ and stays constant thereafter, see the orange line in Fig. 5. Thus, the number
 422 of offspring produced is the same for both development strategies.

423 If cell differentiation is costless ($d_s = d_g = 0$), then the cell doubling time depends only
 424 on the fraction of soma-role cells. As all soma-role cells are then present already after the
 425 first cell division, organisms following the RSD strategy D' will grow faster than organisms
 426 using the ISD strategy D at any stage of organism development, independently of the choice
 427 of the composition effect profile (F_{comp}). At the end of the life cycle, both strategies have
 428 the same expected number of offspring. Therefore, under costless cell differentiation, for any
 429 ISD strategy, we can find a RSD strategy that leads to a larger population growth rate.

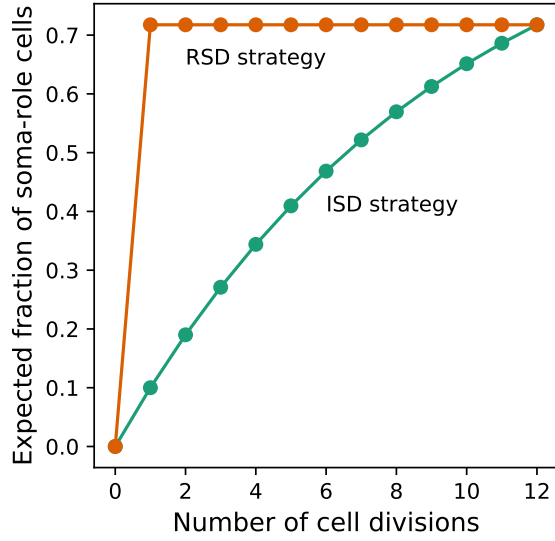


Figure 5: Under costless differentiation, for any irreversible somatic differentiation strategy, exists a reversible somatic differentiation strategy dominating it. The green curve shows the dynamics of the expected fraction of soma-role cells in an organism using an ISD developmental strategy ($m_g = 0.1$, $m_s = 0.0$, $n = 12$). The orange curve shows the dynamics of the expected fraction of soma-role cells in an organism using the specific RSD developmental strategy [$m'_g = 1 - (1 - m_g)^{12} \approx 0.72$, $m'_s = 1 - m'_g \approx 0.28$]. In this strategy, the number of offspring produced at the end of the life cycle is the same as in the considered ISD strategy. At the same time, the fraction of soma-role cells during the life cycle is larger. Therefore, under costless differentiation, the presented RSD strategy is more effective than the considered ISD strategy.

430 **A.3 Conditions promoting the evolution of ISD, RSD, and NSD strate-
431 gies**

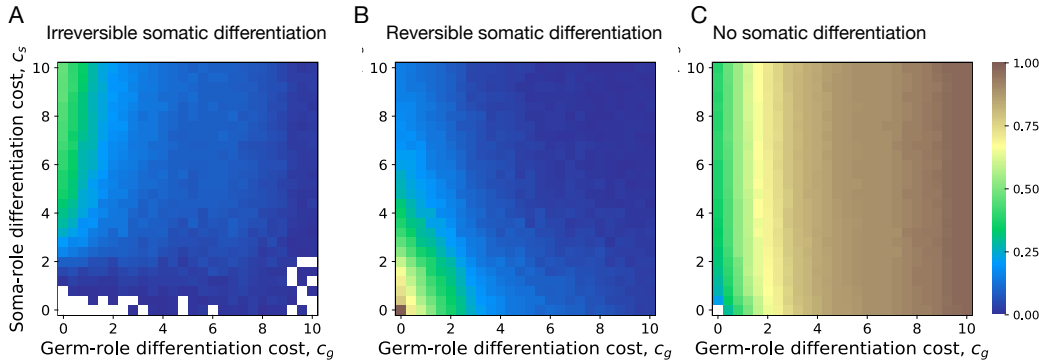


Figure 6: **Impact of cell differentiation costs on the evolution of development strategies.** The fractions of 200 random composition effect profiles promoting ISD (A), RSD (B), and NSD (C) strategies at various cell differentiation costs (c_s , c_g). In the absence of costs ($c_g = c_s = 0$), only RSD strategies were observed. RSD strategies are prevalent at smaller cell differentiation costs. NSD strategies are the most abundant at large costs for germ-role cells (c_g). ISD strategies are the most abundant at large costs for soma-role cells (c_s). The maturity size used in the calculation is 2^{10} cells.

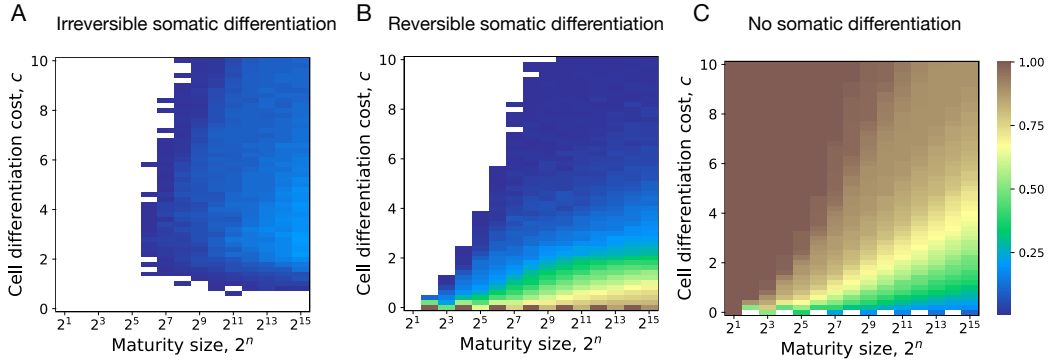


Figure 7: Impact of maturity size on the evolution of development strategies. The fractions of 200 random composition effect profiles promoting ISD (A), RSD (B), and NSD (C) strategies at various cell differentiation costs ($c = c_s = c_g$) and maturity size 2^n . ISD strategies are most abundant at large maturity sizes and intermediary cell differentiation costs. RSD strategies are most abundant at small cell differentiation costs. NSD strategies are most abundant at small maturity sizes and cell differentiation costs.

432 **A.4 Parameters of composition effect profiles promoting ISD, RSD, and**
 433 **NSD strategies**

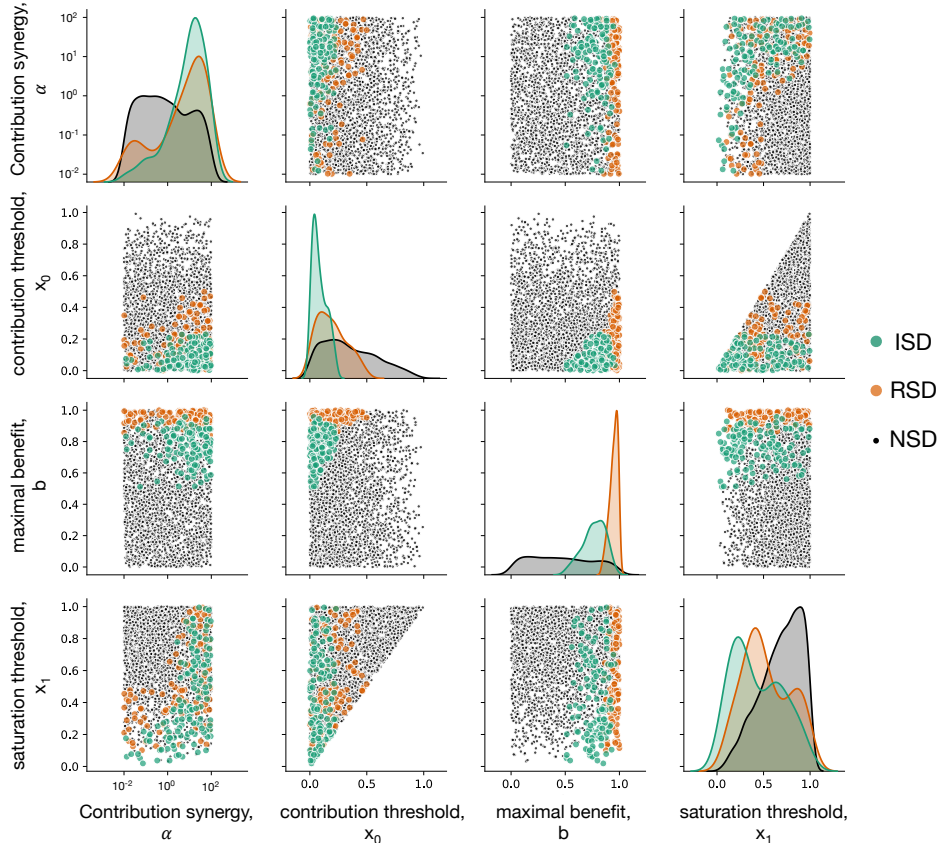


Figure 8: **Impact of composition effect parameters on the evolution of development strategies.**

Each diagonal panel represents individual distribution of each of four parameters among composition effect profiles promoting ISD (green), RSD (orange), and NSD (black) strategies. Each non-diagonal panel represents a pairwise co-distribution of these parameters. ISD strategies are promoted at small contribution thresholds x_0 and for large maximal benefit b . Also, either the contribution synergy α must be large, or the saturation threshold x_1 should be small - see main text for detailed discussion. RSD strategies require very large b - there the benefits of having a large number of soma-role cells outweighs costs paid by frequent differentiation. Due to the fast accumulation of soma-role cells, RSD strategies tolerate larger x_0 than ISD. RSD exhibit the same restrictions with respect to x_1 as ISD and are insensitive to α . For this figure, 3000 composition effect profiles were investigated with costs $c = c_s = c_g = 5$ and $n = 10$.

434 **A.5 Evolution of irreversible somatic differentiation under various ma-**
 435 **turity sizes and unequal cell differentiation costs**

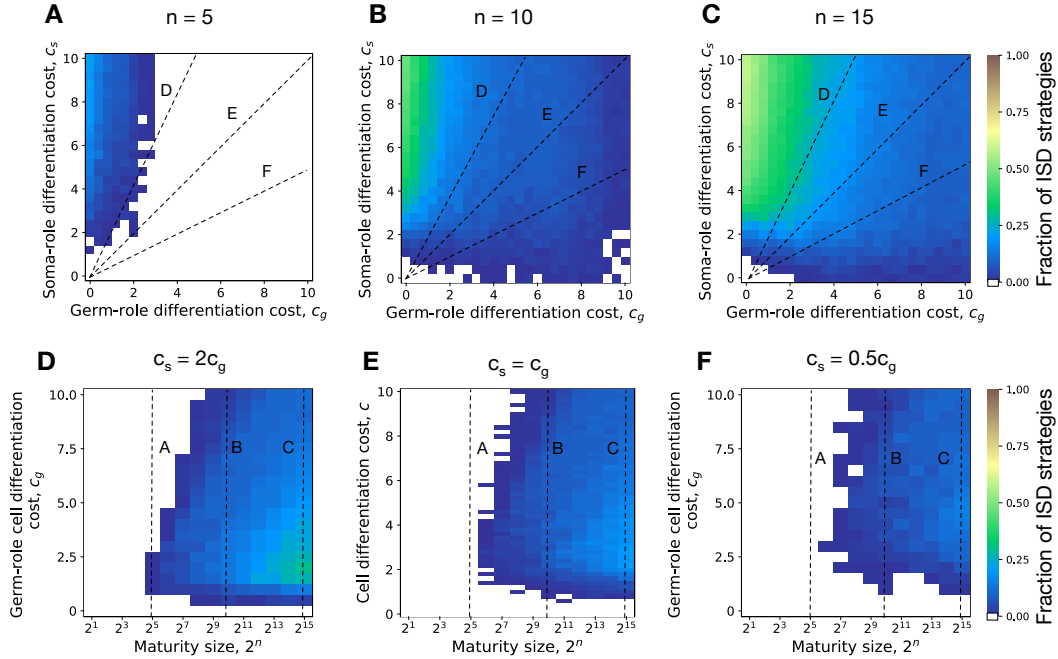


Figure 9: **Evolution of irreversible somatic differentiation at unequal cell differentiation costs.**

A-C. The fraction of 200 random composition effect profiles promoting ISD at various cell differentiation costs (c_s, c_g) at fixed maturity size $n = 5$ (panel A), 10 (B), and 15 (C). Larger maturity sizes promote the evolution of ISD across all cell differentiation costs. **D-F.** The fraction of composition effect profiles promoting ISD at unequal cell differentiation costs $c_s/c_g = 2$ (panel D), $c_s/c_g = 1$ (E), and $c_s/c_g = 0.5$ (F). Even with unequal differentiation costs, the minimal maturity size allowing the evolution of ISD stays roughly the same — $2^5 - 2^6$ cells. Dashed lines indicate overlap between panels.

436 **References**

437 André Amado, Carlos Batista, and Paulo RA Campos. A mechanistic model for the evolution
 438 of multicellularity. *Physica A: Statistical Mechanics and its Applications*, 492:1543–1554,
 439 2018.

440 D. Bakthavatsalam and R.H. Gomer. The secreted proteome profile of developing dictyostelium discoideum cells. Proteomics, 10(13):2556 – 2559, 2010.

441

442 Sean B Carroll. Chance and necessity: the evolution of morphological complexity and diver-
443 sity. Nature, 409(6823):1102, 2001.

444 G.A. Cooper and S. A. West. Division of labour and the evolution of extreme specialization.
445 Nature ecology & evolution, 2018.

446 M. Czarna, G. Mathy, A. MacCord, R. Dobson, W. Jarmuszkiewicz, C.M. Sluse-Goffart,
447 P. Leprince, E. De Pauw, and F.E. Sluse. Dynamics of the dictyostelium discoideum mito-
448 chondrial proteome during vegetative growth, starvation and early stages of development.
449 Proteomics, 10(1):6 – 22, 2010.

450 T.Q. DuBuc, C.E. Schnitzler, E. Chrysostomou, E.T. McMahon, Febrimarsa, J.M. Gahan,
451 T. Buggie, S.G. Gornik, S. Hanley, S.N. Barriera, P. Gonzalez, A.D. Baxevanis, and
452 U. Frank. Transcription factor ap2 controls cnidarian germ cell induction. Science, 367
453 (6479):757–762, 2020.

454 E.Y. Erten and H. Kokko. From zygote to a multicellular soma: body size affects optimal
455 growth strategies under cancer risk. Evolutionary Applications, 13(7):1593 – 1604, 2020.

456 RM Fisher, T Bell, and S A West. Multicellular group formation in response to predators in
457 the alga chlorella vulgaris. Journal of evolutionary biology, 29(3):551–559, 2016.

458 J.R. Gallon. Tansley review no. 44. reconciling the incompatible: N2 fixation and o2. New
459 Phytologist, pages 571–609, 1992.

460 Y. Gao, A. Traulsen, and Y. Pichugin. Interacting cells driving the evolution of multicellular
461 life cycles. PLoS Computational Biology, 15(5):e1006987, 2019.

462 S. Gavrillets. Rapid transition towards the division of labor via evolution of developmental
463 plasticity. PLoS Computational Biology, 6(6):e1000805, 2010.

464 465 466 467 468 469 470 471 472 473 474 475 476 477 478 479 480 481 482 483 484 485 486 487

Heather J Goldsby, Anna Dornhaus, Benjamin Kerr, and Charles Ofria. Task-switching costs promote the evolution of division of labor and shifts in individuality. Proceedings of the National Academy of Sciences, 109(34):13686–13691, 2012.

Heather J Goldsby, David B Knoester, Benjamin Kerr, and Charles Ofria. The effect of conflicting pressures on the evolution of division of labor. PloS one, 9(8):e102713, 2014.

R. K. Grosberg and R. R. Strathmann. One cell, two cell, red cell, blue cell: the persistence of a unicellular stage in multicellular life histories. Trends in ecology & evolution, 13(3): 112 – 116, 1998.

Richard K Grosberg and Richard R Strathmann. The evolution of multicellularity: A minor major transition? Annual Review of Ecology, Evolution, and Systematics, 38:621–654, 2007.

A. Hallmann. Evolution of reproductive development in the volvocine algae. sexual plant reproduction, 24(2):97 – 112, 2011.

Teppo Hiltunen and Lutz Becks. Consumer co-evolution as an important component of the eco-evolutionary feedback. Nature Communications, 5:5226, 2014.

Iaroslav Ispolatov, Martin Ackermann, and Michael Doebeli. Division of labour and the evolution of multicellularity. Proceedings of the Royal Society of London B: Biological Sciences, 279(1734):1768–1776, 2012.

K. Kikuchi. Cellular differentiation in *pleodorina californica*. Cytologia, 43(1):153 – 160, 1978.

D. L. Kirk. A twelve step program for evolving multicellularity and a division of labor. BioEssays, 27(3):299–310, 2005.

V. Koufopanou. The evolution of soma in the volvocales. The American Naturalist, 143(5): 907 – 931, 1994.

488 Robert Lanfear. Do plants have a segregated germline? Do plants have a segregated
489 germline?, 16(5):e2005439, 2018.

490 H.J. Marchant. Colony formation and inversion in the green alga *eudorina elegans*.
491 Protoplasma, 93(2-3):325 – 339, 1977.

492 Gavriel Matt and James Umen. Volvox: A simple algal model for embryogenesis, morpho-
493 genesis and cellular differentiation. Developmental biology, 419(1):99–113, 2016.

494 Carsten Matz and Staffan Kjelleberg. Off the hook–how bacteria survive protozoan grazing.
495 Trends in Microbiology, 13(7):302–307, 2005. doi: 10.1016/j.tim.2005.05.009.

496 Richard E Michod. Evolution of individuality during the transition from unicellular to multi-
497 cellular life. Proceedings of the National Academy of Sciences, 104(suppl 1):8613–8618,
498 2007.

499 K.V. Mikhailov, A.V. Konstantinova, M.A. Nikitin, P.V. Troshin, L.Y. Rusin, V.A. Lyubetsky,
500 Y.V. Panchin, A.P. Mylnikov, L.L. Moroz, S. Kumar, and V.V. Aleoshin. The origin of
501 metazoa: a transition from temporal to spatial cell differentiation. Bioessays, 31(7):758 –
502 768, 2009.

503 Julie Morand-Ferron and John L Quinn. Larger groups of passerines are more efficient prob-
504 lem solvers in the wild. Proceedings of the National Academy of Sciences, 108(38):15898–
505 15903, 2011.

506 S.Y. Ow, T. Cardona, A. Taton, A. Magnuson, P. Lindblad, K. Stensjo, and P.C. Wright.
507 Quantitative shotgun proteomics of enriched heterocysts from *nostoc* sp. pcc 7120 using
508 8-plex isobaric peptide tags. Journal of Proteome Research, 7(4):1615 – 1628, 2008.

509 Y. Pichugin, J. Peña, P.B. Rainey, and A. Traulsen. Fragmentation modes and the evolution
510 of life cycles. PLoS Computational Biology, 13(11):e1005860, 2017.

511 511 W. C Ratcliff, R. F Denison, M Borrello, and M Travisano. Experimental evolution of mul-
512 512 ticellularity. *Proceedings of the National Academy of Sciences USA*, 109(5):1595–1600,
513 513 Jan 2012.

514 514 João F Matias Rodrigues, Daniel J Rankin, Valentina Rossetti, Andreas Wagner, and Homay-
515 515 oun C Bagheri. Correction: Differences in Cell Division Rates Drive the Evolution of
516 516 Terminal Differentiation in Microbes. *PLoS computational biology*, 8(5), 2012.

517 517 Valentina Rossetti, Bettina E Schirrmeister, Marco V Bernasconi, and Homayoun C Bagheri.
518 518 The evolutionary path to terminal differentiation and division of labor in cyanobacteria.
519 519 *Journal of Theoretical Biology*, 262(1):23–34, 2010.

520 520 C. Rueffler, Joachim Hermisson, and Günther P. Wagner. Evolution of functional specializa-
521 521 tion and division of labour. *Proceedings of the National Academy of Sciences USA*, 109:
522 522 E326–E335, 2012.

523 523 A.V.S.S. Sambamurty, editor. *A textbook of algae*. IK International Pvt. Limited, 2005.

524 524 G. Sandh, M. Ramstrom, and K. Stensjo. Analysis of the early heterocyst cys-proteome in the
525 525 multicellular cyanobacterium *nostoc punctiforme* reveals novel insights into the division of
526 526 labor within diazotrophic filaments. *BMC Genomics*, 15(1):1064, 2014.

527 527 Deborah E Shelton, Alexey G Desnitskiy, and Richard E Michod. Distributions of repro-
528 528 ductive and somatic cell numbers in diverse *volvox* (chlorophyta) species. *Evolutionary
529 529 ecology research*, 14:707, 2012.

530 530 Cristian A Solari, John O Kessler, and Raymond E Goldstein. A general allometric and life-
531 531 history model for cellular differentiation in the transition to multicellularity. *The American
532 532 Naturalist*, 181(3):369–380, 2013.

533 533 D. Tverskoi, V. Makarenkov, and F. Alekserov. Modeling functional specialization of a cell
534 534 colony under different fecundity and viability rates and resource constraint. *PLOS ONE*,
535 535 13(8):e0201446, 2018.

536 James S Waters, C Tate Holbrook, Jennifer H Fewell, and Jon F Harrison. Allometric scaling
537 of metabolism, growth, and activity in whole colonies of the seed-harvester ant pogono-
538 myrmex californicus. The American Naturalist, 176(4):501–510, 2010.

539 Martin Willensdorfer. On the evolution of differentiated multicellularity. Evolution, 63(2):
540 306–323, 2009.

541 M.J. Wynne and H.C. Bold. Introduction to the Algae: Structure and Reproduction. Prentice-
542 Hall, Incorporated, 1985.